HHS Public Access

Author manuscript

Bipolar Disord. Author manuscript; available in PMC 2016 April 19.

Published in final edited form as:

Bipolar Disord. 2016 February ; 18(1): 41–51. doi:10.1111/bdi.12364.

Differential effect of lithium on cell number in hippocampus and prefrontal cortex in adult mice: a stereological study

G. Rajkowska[1,*], **G. Clarke**[1,2], **G. Mahajan**[1], **C.M.M. Licht**[3,4], **H.J.J. M. van de Werd**[3], **P. Yuan**[5], **C.A. Stockmeier**[1], **H.K. Manji**[5,6], and **H.B.M. Uylings**[3,*]

[1]Dept. Psychiatry and Human Behavior, University of Mississippi Medical Center, Jackson, MS, USA [2]Department of Psychiatry and Alimentary Pharmabiotic Centre, University College Cork, Cork, Ireland [3]Dept. Anatomy & Neuroscience, VU University Medical Center, Amsterdam, the Netherlands [4]Dept. Epidemiology & Biostatistics, VU University Medical Center, Amsterdam, the Netherlands [5]Laboratory of Molecular Pathophysiology and Experimental Therapeutics, NIMH, NIH, Bethesda, MD, USA [6]Janssen Research and Development LLC of Johnson & Johnson, Titusville, NJ, USA

Abstract

Objectives—Neuroimaging studies note lithium-related increases in the volume of gray matter in prefrontal cortex (PFC) and hippocampus. Postmortem human studies report alterations in neuronal and glial cell density and size in the PFC of lithium-treated subjects. Rodents treated with lithium exhibit cell proliferation in the dentate gyrus (DG) of the hippocampus. However, it is not known whether hippocampal and PFC volume are also increased in these animals or whether cell number in the PFC is altered.

Methods—Using stereological methods, this study estimated the total number of neurons, glia and the packing density of astrocytes in the DG and PFC of normal adult mice treated with lithium and evaluated the total volume of these regions and the entire neocortex.

Results—Lithium treatment increased the total number of neurons and glia in the DG (25% and 21%, respectively) and the density of astrocytes but did not alter the total number in the PFC. However, the volume of the hippocampus and its subfields, the PFC and its subareas, and the entire neocortex were not altered by lithium.

Conclusions—Both neuronal and glial cells accounted for lithium-induced cell proliferation in the DG. That the number of neurons and glia were unchanged in the PFC is consistent with the view that this region is not a neurogenic zone. Further studies are required to clarify the impact of lithium treatment on the PFC under pathological conditions and to investigate the dissociation between increased cell proliferation and unchanged volume in the hippocampus.

Correspondence: Grazyna Rajkowska Ph.D. Dept. Psychiatry and Human Behavior, University of Mississippi Medical Center, 2500 North State street Jackson, MS, 39216, USA; Fax: 601-984-5899; grajkowska@umc.edu.
*These authors contributed equally.

Disclosure

The authors of this paper report no biomedical financial interests or potential conflicts of interest in connection with this manuscript. HKM is a full-time employee of Janssen Pharmaceuticals/Johnson & Johnson: all of this work was conducted while he was an employee of the National Institute of Mental Health.

Keywords

lithium; neurons; glia; astrocytes; stereology; bipolar disorder; adult neurogenesis

INTRODUCTION

Studies of postmortem tissues in subjects with bipolar disorder (BD) have found reductions in the density of neurons and glia as well as smaller neuronal cell bodies in the prefrontal cortex (PFC) (1, 2). In contrast, significantly larger glial nuclei and width of PFC layer III were observed in subjects with BD (1). Many of the subjects included in these studies were treated with lithium, a mood stabilizing drug; thus, it is unclear whether the profile of cellular alterations observed postmortem is a consequence of lithium treatment or a pathological feature of BD *per se*.

Lithium has neuroprotective effects, in addition to its use as a therapeutic or augmentation agent in treating BD (3–7). For example, in BD patients, lithium treatment increases the volume of the cortex, total 'brain' gray matter, prefrontal gray matter, subgenual prefrontal gray matter (3, 4, 8), and bilateral hippocampal volume (9, 10). Interestingly, in healthy individuals, lithium treatment did not alter total gray matter volume, but four weeks of therapeutic doses of lithium increased gray matter density in the PFC (11). These observations are in line with a recent magnetic resonance imaging (MRI) study in adult male Sprague-Dawley rats that noted that total brain volume and cortical gray matter (including the frontal cortex) were increased after four weeks of lithium treatment, but no significant increase occurred in hippocampal volume (12). In adult mice, chronic administration of lithium promotes the proliferation of new cells in the hippocampus, as noted with bromodeoxyuridine (BrdU) immunohistochemistry (13); however, the phenotype of these newly-generated cells has only partially been determined (13). Moreover, two other reports on lithium-induced neurogenesis in normal adult rat dentate gyrus and embryonic hippocampal rat tissue culture revealed that the phenotype of newly born cells was neuronal (14, 15).

The present study sought to establish which type of brain cells (neurons, glia and/or astrocytes) are involved in cell proliferation associated with lithium in mice. Moreover, since the medial PFC (mPFC) has not been studied in this context in a rodent model, we examined the effects of lithium treatment on the volume of mPFC and hippocampal areas, in addition to a stereological analysis of neuronal and glial total cell number and astrocyte density in these regions. The study used normal adult mice to investigate two main questions. First, whether lithium treatment at therapeutically relevant doses affects the total number of neurons and glia, and/or the packing density of astrocytes in the mPFC and hippocampal areas. Second, whether lithium treatment alters the volume of the mPFC, hippocampal areas, or the entire neocortex.

Materials and Methods

1. Animals and histological processing

Twenty adult, male mice (strain C57BL/6) of similar weight (± 20g) were randomly divided into two groups: a lithium-treated group (n=10) and a control, placebo-treated group (n=10). Mice were chronically treated with lithium or placebo at the National Institute of Mental Health (Bethesda, MD, USA) using standard procedures as previously reported (13). All animal procedures were conducted in strict accordance with the animal care guidelines of the National Institutes of Health and were approved by a local animal ethics committee. The mice were treated for four weeks with control or lithium chow (2.4 g/kg of Li_2CO_3) at a dose that achieved plasma lithium levels similar to therapeutic doses for BD (0.6–1.2mM).

The histological processing of the brains of lithium-treated and control mice was performed at the Department of Psychiatry and Human Behavior, University of Mississippi Medical Center, Jackson, USA. Mouse brains were embedded in celloidin (as previously described in 16, 17, and adapted for mouse brain). Celloidin was chosen as an embedding medium for preparing thick sections with clear morphology and high contrast of stained neurons and glial cells (18). A complete series of coronal 40μm thick sections was cut from each brain using an electronic sliding microtome. Sections were stained with cresyl violet (Nissl method) or immunohistochemically processed for microscopic analysis. Two series of sections per brain were prepared for examination: one series contained the even-numbered sections and the other contained the odd numbered sections. One series was used for cell counting and immunohistochemistry at the University of Mississippi Medical Center, and the other series for volumetric analysis at the VU University Medical Center, Amsterdam.

In addition, in 6 animals per group, 4–6 sections from the PFC and the dentate gyrus were collected adjacent to Nissl sections and were stained with immunohistochemistry for GFAP-immunoreactive astrocytes. Celloidin was removed from the selected sections (19) which were then incubated with anti-GFAP mouse monoclonal antibody (1:500, Sigma) in accordance with a previous protocol (20) that was adapted for mouse brain.

2. Stereological methods

Stereological methods were used to estimate the total cell number and volume of the hippocampus and mPFC and the volume of the entire neocortex in both groups of mice. In addition, the 3-dimensional cell packing density of astrocytes was estimated in 6 animals per group. StereoInvestigator software (v.8, MicroBrightField Bioscience, Williston, VT) was used to carry out these analyses. Brain sections were coded to permit collection of cell parameters under blinded conditions.

2.1. Total number of neurons and glia—The total number of neurons and glial cells was estimated in the entire mPFC and the dentate gyrus (DG) of the hippocampus in the left hemisphere (Fig. 1). We applied previously validated cytoarchitectonic criteria to delineate the DG (21, 22). The criteria for delineating the mouse mPFC (i.e., the infralimbic area (IL) plus the prelimbic area (PL) plus the ventral anterior cingulate area (ACv) plus the dorsal anterior cingulate area (ACd) plus the frontal area 2 (Fr2)) were previously reported (23,

24). Cell counting was performed in only one hemisphere because no significant differences were found between hemispheres with regard to mPFC or DG volume. Neurons were distinguished from glial cells by having much larger cell bodies, different appearance of the chromatin within the nucleus, and presence of nucleolus and visible cytoplasm around nuclei (25, 26) (Fig. 2). We did not distinguish between different types of glial cells (i.e. astrocytes, oligodendrocytes and microglia) as it is difficult and not reliable in Nissl-stained material. However, we identified astrocytes on adjacent sections by using immunohistochemistry with a specific anti-GFAP antibody in 12 animals.

The optical fractionator method (27) was applied to estimate the total number of Nissl-stained neurons and glial cells. In each animal, six to 12 sections at a fixed 160–200 μm interval were systematically randomly sampled from the mPFC and DG. A Leica stereomicroscope and Nikon 600-N research microscope were used to delineate the boundaries of the mPFC and DG in each of these sections using the cytoarchitectonic criteria described above with (Fig. 1). Within these boundaries, 3-D optical disector probes were positioned in a systematic random way using a 100X oil immersion objective with a numerical aperture of 1.4. The dimensions of the optical disector box were 30 × 30 X 25 μm for the mPFC cells, 15 × 15 X 25 μm for the DG neurons, and 40 × 40 X 25 μm for the DG glial cells. In each animal, 359–777 neurons and 176–381 glial cells were sampled from all disector probes (Σ Q) within the mPFC, and 170–290 neurons and 150–320 glial cells within the DG. No correction for histological shrinkage was applied because the stereological estimate of the total cell number in the celloidin sections is not affected by tissue shrinkage (e.g., 27). All 20 mice were included in the analysis of cell number in the DG and in the mPFC.

The precision of the ‘optical fractionator’ in estimating cell number per animal is expressed by the coefficient of error (CE) and was calculated as $CE^2 \approx 1/\Sigma Q$ (28, 29). In general, this is a good approximation of CE (for details, see 30–32). The variability between the animals per group is indicated by the 95% confidence interval (CI). In addition to the ‘within’-animal variation measure of CE, the observed inter-animal coefficient of variation (CV= SD/mean) was calculated to evaluate study design; a $[CE^2/CV^2] \leq 0.5$ was considered desirable (33). Differences between the lithium-treated and control groups with regard to total number of neurons and glial cells (DG neuron number, DG glial number, mPFC neuron number, mPFC glial number) were tested using repeated measures ANOVA to account for the experimental design. This ANOVA was followed by post-hoc Welch’s t-tests. The Welch’s t-test was applied to account for unequal variances and skewed distributions with the exception of extreme cases (34). For data from the DG, a 1-tailed test was used, since the direction of difference was predicted by our former publication (13)(i.e., higher cell number in DG in the lithium-treated group). For data from the mPFC, a 2-tailed test was applied.

2.2 Density of astrocytes—In addition to estimates of total cell number of Nissl-stained neurons and glia, the packing density of GFAP-immunoreactive astrocytes was estimated on adjacent sections in 6 animals per group. Four to 6 sections per animal were systematically sampled with a fixed inter-slide interval of 300–400μm from the mPFC and DG in the left hemisphere. Limited availability of sections prevented sampling a larger number of sections; hence, astrocyte density and not total number was estimated. The boundaries of the mPFC

and DG were delineated in each of these immuno-stained sections by imposing cytoarchitectonic boundaries of these regions from adjacent Nissl-stained sections. The optical fractionator method with 3-dimensional disector box was used as described above. The dimensions of the optical disector box were 40 × 40 X 15 μm and there were 28–35 disector boxes per brain region. The packing density of astrocytes was calculated as the sum of cells counted within all disectors divided by the volume of all disectors. The average density per region per brain was compared between the two groups of animals by Welch's t test.

2.3 Volume estimation—The volumes of the hippocampus and its subfields, the mPFC and its subareas, and the entire neocortex were measured in another series of sections (see above) in both left and right hemispheres using the Cavalieri principle (30, 33, 35). The following subfields were measured separately: in the hippocampus, the areas of the Cornu Ammonis (CA1, CA2+3), the DG, the hilus, and the subiculum; in the mPFC: IL, PL, ACv, ACd, and Fr2 (23, 24).

In a set of systemically random sampled sections (about six to 20 sections per brain region), the different brain areas were microscopically delineated using a Zeiss research microscope under 25X-60X magnification. The IBAS Kontron image analysis system (Munich, Germany) was used for surface area measurements of the delineated subfields in the sections sampled. The volume was estimated based on cross-sectional area measurements using Cavalieri's principle (for details, see 30, 35). The thickness of the sections of each mouse studied was measured with a 63x high-power oil-immersion objective with a numerical aperture of 1.25 (35). No correction for histological shrinkage was applied. Due to local artefacts in some sections, 19 out of 20 mice were used for volumetric analysis of the mPFC, and 16 out of 20 mice for volumetric analysis of the whole neocortex and hippocampus in both hemispheres.

The precision of volume estimations per animal (CE) is expressed by Gundersen and Jensen's quadratic approximation formula (36, 37). In this equation we applied m=0; m is the smoothness constant of the cross-sectional area function of the object studied (e.g., 30). This results in a conservative estimate of CE with $\alpha = 1/12$, which generally closely matches the resampling estimates of CE (37, 38). The coefficient, α, is a function of the smoothness constant m (39). Analysis of the differences in volume of hippocampal subfields, mPFC, and neocortex between the lithium-treated and control groups was performed using repeated measures ANOVA tests (SPSS software). In addition, the lateralisation ratios, $\mathrm{LR}=\frac{(L-R)}{(L+R)}$, were tested (30). To correct the volume of the hippocampus, mPFC, and their subareas for the total neocortex volume and the DG volume for total hippocampal volume, adjusted predicted values were calculated using regression analysis. One-way ANOVAs were performed on these adjusted values.

RESULTS

Cell number

The mean value estimates for the total number of Nissl-stained neurons and glial cells, with their 95% confidence intervals, are presented in Table 1.

Repeated measures ANOVA revealed significant interactions between the number of cells—that is, number of neurons in the DG, number of glial cells in the DG, number of neurons in the mPFC, and number of glial cells in the mPFC—and the groups ($F(3, 54)=4.362$, $p<0.01$). This analysis demonstrates a highly significant difference in hippocampal and mPFC cell number due to lithium treatment. This significant differential result in cell number due to lithium was determined by post-hoc analyses. The total number of Nissl-stained glial cells in the dentate gyrus of the hippocampus was significantly increased by 21% ($t=2.13$, $df=15.23$, $p=0.025$) in lithium-treated mice compared to control mice (Table 1, Fig. 3A). In the lithium-treated group, the total number of neurons in the DG was significantly increased by 25% compared to the control group ($t= 1.98$, $df=16.11$, $p<0.05$) (Table 1, Fig. 3B). In addition, both the mean of the total number of neurons and the mean of the total number of glial cells in the DG of the control group are outside the 95% confidence interval of the lithium-treated group and vice versa (Table 1). In contrast to the DG, in the mPFC, no significant differences were observed between lithium-treated and control groups in the number of glial ($t=1.44$, $df=17.36$, $p=0.18$) or neurons ($t=0.86$, $df=16.13$, $p=0.40$) (Table 1, Fig. 4). Means of the total number of neurons and glia in the mPFC of the control group are within the 95% confidence interval of the lithium-treated group and vice versa (Table 1). The precision of estimating the stereological total cell number per animal (CE) was sufficient with respect to the inter-animal variation (CV), since all $[CE^2/CV^2] < 0.5$ (Table 1).

Cell density

The density of GFAP-immunoreactive astrocytes was significantly increased by 15% ($t=2.95$, $df=8.97$, $p<0.01$) in the DG in the lithium-treated mice as compared to control mice (Fig. 5A). In contrast, in the mPFC, no significant differences in astrocyte density ($t=0.054$, $df=7.20$, $p=0.96$) were observed between the groups (Fig. 5B).

Volume analysis

No significant differences were found in the volume of any of the main cortical regions (mPFC, hippocampus, entire neocortex) between the hemispheres or between the lithium-traeated and control groups (all *p*-values > 0.05) (see Tables 2, 3, and Fig. 6). Volumetric analyses of individual hippocampal subfields and mPFC subareas revealed a significant difference in only one mPFC subdivision: the ACv area in the left hemisphere ($df=17$, $t= -2.150$, $p< 0.05$). The volume of this subregion was larger in the treated group compared with the control group. However, this difference did not remain significant after Bonferroni correction for multiple comparisons ($p=0.05/13 = 0.004$). For only one mPFC subdivision (i.e., the ACv area) the mean value of the control group was outside the 95% confidence interval of the lithium-treated group and vice versa (Tables 2,3). The stereological precision of volume estimation per animal relative to the inter-animal variation was sufficient for all

the main cortical regions and all subfields, except for a few hippocampal subfields (Tables 2, 3). No significant group differences were detected using one-way ANOVA of the predicted values of the volume of the hippocampus and mPFC adjusted for the total neocortex volume. In addition, no significant group difference was found for the predicted values of the DG volume adjusted for the total hippocampal volume.

Discussion

This study revealed significant increases in the total number of neurons and glial cells and in astrocyte density in the DG of the hippocampus of adult mice treated with lithium, as compared to control animals. In contrast, in the mPFC of the same animals, no significant changes were observed in the lithium-treated group in either total number of neurons or glial cells or in astrocyte density. No significant volumetric differences were seen between the groups for any of the regions studied (mPFC, hippocampus, entire neocortex). The observed increase in cell number in the DG of lithium-treated mice is consistent with results from a previous study using the same strain of mice showing that lithium increased the number of newly formed (BrdU-labeled) cells in the DG (13). Two other studies report a similar magnitude of lithium-induced increases in BrdU-labeled cells in normal rat dentate gyrus and in rat embryonic hippocampal cell culture (14, 15). The newly added cells in both of these studies were identified as neurons. However, the present study suggests that both cellular phenotypes, neurons and glial cells (including astrocytes) account for lithium-induced cell proliferation in the DG. In contrast to the effect of lithium in the DG, in mPFC we observed that neither the number of neurons nor of glial cells were significantly changed in response to lithium. This regional difference in response to lithium is consistent with the view that mPFC is not a neurogenic zone. From the current study, it cannot be determined if the lack of lithium-induced increases in cell numbers in the mPFC is related to a lack of cell proliferation, to low cell proliferation below detectable levels (40), or to low survival rates of newborn neurons/glia. Interestingly, region-specific effects of chronic lithium on the expression of histone deacetylases have consequent implications for neurogenesis (41, 42). Chronic treatment of mice with lithium reduced the expression of several isoforms of Class I and II histone deacetylase (HDAC) in hippocampus but not in cingulate cortex (41). HDAC family members affect neurogenesis by playing crucial roles controlling gene expression, cell fate, and activity of transcription factors (42). Thus, our observation of increased neurogenesis in DG in mice treated with lithium (13) may have involved HDAC family members in the hippocampus.

In the present study, several experimentally-derived observations are in line with well-validated criteria. These include the precision of the stereological estimations per animal, the inter-animal variation in total neuron number and total glia number, and the volume of the main cortical regions and their subfields, including the DG. For the volume estimations, we applied a conservative estimate of stereological precision (37, 38), in which CE^2 was 20 times larger than with $\alpha=1/240$, a factor that has been frequently used in previous studies (for details, see 30). With this conservative precision estimate, only a few hippocampal subfields (i.e., hilus, control subiculum, and control CA 2–3 subfields) did not meet the pre-defined criteria ($[CE^2/CV^2] \leq 0.5$). In these few hippocampal subfields, the proportion $[CE^2/CV^2]$ was larger than 0.5 (Table 2) due to a number of different factors including small

inter-animal variation, small volume value, and a smaller number of animals. For this study, it is important to note that the stereological precision for the DG volume estimation was sufficient. In this hippocampal subfield, we detected a significant increase in the number of neurons and glial cells, and no change in its volume.

Our estimates of total neuron number in the DG of control C57BL/6 mice are similar to those published by Kempermann and Gage (43, 44) and Fabricius and colleagues (45), and comparable to estimates made by Boekhoorn and colleagues (46) for C57BL/6 mice. The number of glial cells in the DG was about 1/10 of the neuronal number, which is consistent with estimates made by Kimoto and colleagues (47). Our estimates of glial cell number are comparable to the estimates of astrocyte number made by Mouton and colleagues (48). Because astrocytes form the vast majority of glial cells in the DG (47, 48), it is likely that the increase in glial cell number reflects an increase in the total number of astrocytes. Moreover, the increase in the total number of neurons could also be due to an increase in the number of astrocytes as astrocytes give rise to new neurons in the adult hippocampus (49, 50). Our present observation on the increased packing density of GFAP-immunoreactive astrocytes is consistent with the above hypotheses. The density of GFAP-immunoreactive astrocytes in lithium-treated mice was significantly increased in the DG of the hippocampus but not in the mPFC as compared to control animals, while the volumes of DG and mPFC remained unchanged.

To build upon the results of the present study noting an increased total number of neurons and glia cells in the DG of lithium-treated mice, we conducted a pilot study to examine the size of neuronal somata and glial nuclei. However, lithium had no significant effect on sizes in neurons or glia in the DG. Neuronal somata size is correlated with total dendritic length (e.g., 51). Therefore, our pilot data on somata size corroborate the observations of Seong and colleagues (52) who reported dendritic rearrangements in the DG in lithium-treated mice but no changes in total dendritic length.

Given that our results identified a lithium-induced increase in the total number of neurons and glial cells and increase in density of astrocytes in the DG and no change in cell number in the mPFC, one might predict that lithium would increase the volume of the DG and hippocampus but not of the mPFC. However, our study noted no significant lithium-induced volumetric changes in either the hippocampus or mPFC. This observation is supported by the work of Fabricius and colleagues (45), who reported a significantly altered number of neurons in the DG but no detectable change in DG volume. The dissociation between volume and cell number is an interesting observation that warrants further investigation. Although DG volumes have not been investigated in human studies, the total volume of the entire hippocampus has been reported in individuals with BD. Several studies, including one meta-analysis, found no changes in hippocampal volume in BD patients (53–55). However, other studies reported lithium-related increases in hippocampal volume (9, 10, 56, 57). The discrepancies between studies could be due to small sample size, technical details (e.g., the slice thickness of the MRI), and the clinical heterogeneity of patient populations.

Echoing the lack of effect of lithium on regional volumes in the entire neocortex and individual areas of the mPFC and hippocampus observed in the present study, one meta-

analysis reported no changes in gray matter volume in BD patients treated with lithium (58). In contrast, several other studies reported lithium-related increases in gray matter volume and the volume of individual prefrontal areas in BD patients (3, 4, 8, 11). One explanation for the discrepancy in regional volumes between these clinical studies and the present study is that lithium may have different effects in healthy and diseased brains. In support of this possibility, three studies examining the influence of lithium on brain volume in healthy individuals noted that total gray matter volume remained unchanged (11, 59, 60).

There are limitations to the present study. Lithium was administered to normal mice, as opposed to the MSN strain of mice that display a manic phenotype (61). The specific phenotype of neurons in DG that was increased in number by lithium was not identified. The present study did not determine if the lithium-induced increase in cell numbers in the DG would persist following the cessation of treatment with lithium. The lithium-induced increase in astrocyte density in the DG was only determined in 4–6 sections; the entire hippocampus must be sampled to determine whether lithium increased the total number of astrocytes.

In conclusion, this study found that the total number of both neurons and glial cells was significantly increased in the DG of lithium-treated mice, but remained unchanged in the mPFC. In addition, the packing density of astrocytes was increased in the DG of lithium-treated mice but not significantly affected in the mPFC. Moreover, the volume of the hippocampus and its subfields, the mPFC and its subareas, and the entire neocortex, remained unchanged in lithium-treated animals. Both neurons and glia accounted for lithium-induced cell proliferation in the DG. These findings present a more detailed picture of lithium-induced alterations in DG cellular phenotype than previously available, and the first evidence for lithium-induced increases in glia, in general, and astrocytes, in particular. In contrast, lithium had no significant effect on the number of neurons and glia in the mPFC, suggesting that this region is not a neurogenic zone. Further studies are required to assess the impact of lithium treatment under pathological conditions in this region and to investigate the dissociation between increased cell proliferation and volume in the hippocampus.

Acknowledgements

This work was supported by grants: MH61578 and P30 GM103328.

References

1. Rajkowska G, Halaris A, Selemon LD. Reductions in neuronal and glial density characterize the dorsolateral prefrontal cortex in bipolar disorder. Biol Psychiatry. 2001; 49:741–752. [PubMed: 11331082]
2. Chana G, Landau S, Beasley C, Everall IP, Cotter D. Two-dimensional assessment of cytoarchitecture in the anterior cingulate cortex in major depressive disorder, bipolar disorder, and schizophrenia: evidence for decreased neuronal somal size and increased neuronal density. Biol Psychiatry. 2003; 53:1086–1098. [PubMed: 12814860]
3. Moore GJ, Bebchuk JM, Wilds IB, Chen G, Manji HK. Lithium-induced increase in human grey matter. Lancet. 2000; 356:1241–42. Erratum in: Lancet 2000; 356: 2104. [PubMed: 11072948]

4. Moore GJ, Cortese BM, Glitz DA, Zajac-Benitez C, Quiroz JA, Uhde TW, Drevets WC, Manji HK. A longitudinal study of the effects of lithium treatment on prefrontal and subgenual prefrontal gray matter volume in treatment-responsive bipolar disorder patients. J Clin Psychiatry. 2009; 70:699–705. [PubMed: 19389332]
5. Bauer, M.; Grof, P.; Müller-Oerlingausen, B. Lithium in neuropsychiatry: the comprehensive guide. London: Informa Healthcare; 2006.
6. Schloesser RJ, Martinowich K, Manji HK. Mood-stabilizing drugs: mechanisms of action. Trends Neurosci. 2012; 35:36–46. [PubMed: 22217451]
7. Malhi GS, Tanious M, Das P, Coulston CM, Berk M. Potential Mechanisms of Action of Lithium in Bipolar Disorder Current Understanding. CNS Drugs. 2013; 27:135–153. [PubMed: 23371914]
8. Sassi RB, Nicoletti M, Brambilla P, Mallinger AG, Frank E, Kupfer DJ, Keshavan MS, Soares JC. Increased gray matter volume in lithium treated bipolar disorder patients. Neurosci Lett. 2002; 329:243–245. [PubMed: 12165422]
9. Yucel K, McKinnon MC, Taylor VH, Macdonald K, Alda M, Young LT, MacQueen GM. Bilateral hippocampal volume increases after long-term lithium treatment in patients with bipolar disorder: a longitudinal MRI study. Psychopharmacology. 2007; 195:357–367. [PubMed: 17705060]
10. Yucel K, Taylor VH, McKinnon MC, Macdonald K, Alda M, Young LT, MacQueen GM. Bilateral hippocampal volume increase in patients with bipolar disorder and short-term lithium treatment. Neuropsychopharmacology. 2008; 33:361–367. [PubMed: 17406649]
11. Monkul ES, Matsuo K, Nicoletti MA, Dierschke N, Hatch JP, Dalwani M, Brambilla P, Caetano S, Sassi RB, Mallinger AG, Soares JC. Prefrontal gray matter increases in healthy individuals after lithium treatment: A voxel-based morphometry study. Neurosci Lett. 2007; 429:7–11. [PubMed: 17996370]
12. Vernon AC, Natesan S, Crum WR, Cooper JD, Modo M, Williams SC, Kapur S. Contrasting effects of haloperidol and lithium on rodent brain structure: A magnetic resonance imaging study with postmortem confirmation. Biol Psychiatry. 2012; 71:855–863. [PubMed: 22244831]
13. Chen G, Rajkowska G, Du F, Seraji-Bozorgzad N, Manji HK. Enhancement of hippocampal neurogenesis by lithium. J Neurochemistry. 2000; 75:1729–1734.
14. Son H, Yu IT, Hwang SJ, Kim JS, Lee SH, Lee YS, Kaang BK. Lithium enhances long-term potentiation independently of hippocampal neurogenesis in the rat dentate gyrus. J Neurochem. 2003; 85:872–881. Erratum in: J Neurochem 2003; 85: 1624. [PubMed: 12716419]
15. Kim JS, Chang MY, Yu IT, Kim JH, Lee SH, Lee YS, Son H. Lithium selectively increases neuronal differentiation of hippocampal neural progenitor cells both in vitro and in vivo. J Neurochem. 2004; 89:324–336. [PubMed: 15056276]
16. Rajkowska G, Goldman-Rakic PS. Cytoarchitectonic definition of prefrontal areas in the normal human cortex: IRemapping of areas 9 and 46 using quantitative criteria. Cereb Cortex. 1995; 5:307–322. [PubMed: 7580124]
17. Rajkowska G, Miguel-Hidalgo JJ, Wei J, Dilley G, Pittman SD, Meltzer HY, Overholser JC, Roth BL, Stockmeier CA. Morphometric evidence for neuronal and glial prefrontal cell pathology in major depression. Biol Psychiatry. 1999; 45:1085–1098. [PubMed: 10331101]
18. Uylings HBM, Zilles K, Rajkowska G. Optimal staining methods for delineation of cortical areas and neuron counts in human brains. NeuroImage. 1999; 9:439–445. [PubMed: 10191172]
19. Miguel-Hidalgo JJ, Rajkowska G. Immunohistochemistry of neural markers for the study of the laminar architecture in celloidin sections from the human cerebral cortex. J Neurosci Methods. 1999; 93:69–79. [PubMed: 10598866]
20. Miguel-Hidalgo JJ, Baucom C, Dilley G, Overholser JC, Meltzer HY, Stockmeier CA, Rajkowska G. Glial fibrillary acidic protein immunoreactivity in the prefrontal cortex distinguishes younger from older adults in major depressive disorder. Biol Psychiatry. 2000; 48:861–873. [PubMed: 11063981]
21. West MJ. Stereological studies of the hippocampus: a comparison of the hippocampal subdivisions of diverse species including hedgehogs, laboratory rodents, wild mice and men. Prog Brain Res. 1990; 83:13–36. [PubMed: 2203095]

22. Slomianka L, West MJ. Comparative quantitative study of the hippocampal region of two closely related species of wild mice: Interspecific and intraspecific variations in volumes of hippocampal components. J Comp Neurol. 1989; 280:544–552. [PubMed: 2708565]
23. Van De Werd HJJM, Rajkowska G, Evers P, Uylings HBM. Cytoarchitectonic and chemoarchitectonic characterization of the prefrontal cortical areas in the mouse. Brain Struct Funct. 2010; 214:339–353. [PubMed: 20221886]
24. Van De Werd HJJM, Uylings HBM. Comparison of (stereotactic) parcellations in mouse prefrontal cortex. Brain Struct Funct. 2014; 219:433–459. [PubMed: 24072162]
25. Ling EA, Paterson JA, Privat A, Mori S, Leblond CP. Investigation of Glial Cells in Semithin Sections I Identification of glial cells in the brain of young rats. J Comp Neurol. 1973; 149:43–72. [PubMed: 4121705]
26. Thune JJ, Uylings HBM, Pakkenberg B. Total number of neurons in the prefrontal cortex in schizophrenics and controls. J Psychiatr Res. 2001; 35:15–21. [PubMed: 11287052]
27. West MJ, Slomianka L, Gundersen HJG. Unbiased stereological estimation of the total number of neurons in the subdivisions of the rat hippocampus using optical fractionator. Anat Rec. 1991; 231:482–497. [PubMed: 1793176]
28. Schmitz C. Variation of fractionator estimates and its prediction. Anat Embryol (Berl). 1998; 198:371–397. [PubMed: 9801058]
29. Glaser EM, Wilson PD. The coefficient of error of optical fractionator population size estimates: a computer simulation comparing three estimators. J Microsc. 1998; 192:163–171. [PubMed: 9853373]
30. Uylings HBM, Malofeeva LI, Bogolepova IN, Jacobsen AM, Amunts K, Zilles K. No postnatal doubling of number of neurons in human Broca's area (BA 44 and 45)? A stereological study. Neuroscience. 2005; 136:715–728. [PubMed: 16344146]
31. Cruz-Orive, LM.; Insausti, AM.; Insausti, R.; Crespo, D. A case study from neuroscience involving stereology and multivariate analysis. In: Evans, SM.; Janson, AM.; Nyengaard, JR., editors. Quantitative methods in neuroscience. Oxford: Oxford University Press; 2004. p. 16-64.
32. Cruz-Orive LM. A general variance predictor for Cavalieri slices. J Microsc. 2006; 222:158–165. [PubMed: 16872414]
33. Gundersen HJG. Stereology of arbitrary particles: A review of unbiased number, size estimators presentation of some new ones, in memory of William R Thompson. J Microsc. 1986; 143:3–45. [PubMed: 3761363]
34. Rasch D, Kubinger KD, Moder K. The two-sample *t* test: pre-testing its assumptions does not pay off. Stat Papers. 2011; 52:219–231.
35. Uylings HBM, Van Eden CG, Hofman MA. Morphometry of size/volume variables and comparisons of their bivariate relations in the nervous system under different conditions. J Neurosci Methods. 1986; 18:19–37. [PubMed: 3540468]
36. Gundersen HJG, Jensen EB. The efficiency of systematic sampling in stereology and its prediction. J Microsc. 1987; 147:229–263. [PubMed: 3430576]
37. Gundersen HJG, Jensen EBV, Kiêu K, Nielsen J. The efficiency of systematic sampling in stereology: reconsidered. J Microsc. 1999; 193:199–211. [PubMed: 10348656]
38. Slomianka L, West MJ. Estimators of the precision of stereological estimates: an example based on the CA1 pyramidal cell layer of rats. Neuroscience. 2005; 136:757–767. [PubMed: 16344149]
39. García-Fiñana M, Cruz-Orive LM, Mackay CE, Pakkenberg B, Roberts N. Comparison of MR imaging against physical sectioning to estimate the volume of human cerebral compartments. Neuroimage. 2003; 18:505–516. [PubMed: 12595203]
40. Stanton GB, Kohler SJ, Boklweski J, Cameron JL, Greenough WT. Cytogenesis in the adult monkey motor cortex: Perivascular NG2 cells are the major adult born cell type. J Comp Neurol. 2015; 523:849–868. [PubMed: 25308320]
41. Ookubo M, Kanai H, Aoki H, Yamada N. Antidepressants and mood stabilizers effects on histone deacetylase expression in C57BL/6 mice: Brain region specific changes. J Psychiatr Res. 2013; 47:1204–1214. [PubMed: 23777937]
42. Cho Y, Cavalli V. HDAC signaling in neuronal development and axon regeneration. Curr Opin Neurobiol. 2014; 27:118–126. [PubMed: 24727244]

43. Kempermann G, Gage FH. Experience-dependent regulation of adult hippocampal neurogenesis: effects of long-term stimulation and stimulus withdrawal. Hippocampus. 1999; 9:321–332. [PubMed: 10401646]
44. Kempermann G, Gage FH. Genetic determinants of adult hippocampal neurogenesis correlate with acquisition, but not probe trial performance, in the water maze task. Eur J Neurosci. 2002; 16:129–136. [PubMed: 12153537]
45. Fabricius K, Wörtwein G, Pakkenberg B. The impact of maternal separation on adult mouse behaviour and on the total neuron number in the mouse hippocampus. Brain Struct Funct. 2008; 212:403–416. [PubMed: 18200448]
46. Boekhoorn K, van Dis V, Goedknegt E, Sobel A, Lucassen PJ, Hoogenraad CC. The microtubule destabilizing protein stathmin controls the transition from dividing neuronal precursors to postmitotic neurons during adult hippocampal neurogenesis. Dev Neurobiol. 2014; 74:1226–1242. [PubMed: 24909416]
47. Kimoto H, Eto R, Abe M, Kato H, Araki T. Alterations of glial cells in the mouse hippocampus during postnatal development. Cell Mol Neurobiol. 2009; 29:1181–1189. [PubMed: 19472050]
48. Mouton PR, Long JM, Lei DL, Howard V, Jucker M, Calhoun ME, Ingram DK. Age and gender effects on microglia and astrocyte numbers in brains of mice. Brain Res. 2002; 956:30–35. [PubMed: 12426043]
49. Seri B, García-Verdugo JM, McEwen BS, Alvarez-Buylla A. Astrocytes give rise to new neurons in the adult mammalian hippocampus. J Neurosci. 2001; 21:7153–7160. [PubMed: 11549726]
50. Song H, Stevens CF, Gage FH. Astroglia induce neurogenesis from adult neural stem cells. Nature. 2002; 417:39–44. [PubMed: 11986659]
51. Uylings HBM, Van Pelt J. Measures for quantifying dendritic arborizations. Network: Computation in Neural Systems. 2002; 13:397–414.
52. Seong SS, Hammonds MD, Mervis RF. Four weeks lithium treatment alters neuronal dendrites in the rat hippocampus. Int J Neuropsychopharmacol. 2013; 16:1373–1382. [PubMed: 23331381]
53. Altshuler LL, Bartzokis G, Grieder T, Curran J, Jimenez T, Leight K, Wilkins J, Gerner R, Mintz J. An MRI study of temporal lobe structures in men with bipolar disorder or schizophrenia. Biol Psychiatry. 2000; 48:147–162. [PubMed: 10903411]
54. McDonald C, Zanelli J, Rabe-Hesketh S, Ellison-Wright I, Sham P, Kalidindi S, Murray RM, Kennedy N. Meta-analysis of magnetic resonance imaging brain morphometry studies in bipolar disorder. Biol Psychiatry. 2004; 56:411–417. [PubMed: 15364039]
55. Strasser HC, Lilyestrom J, Ashby ER, Honeycutt NA, Schretlen DJ, Pulver AE, Hopkins RO, Depaulo JR, Potash JB, Schweizer B, Yates KO, Kurian E, Barta PE, Pearlson GD. Hippocampal and ventricular volumes in psychotic and nonpsychotic bipolar patients compared with schizophrenia patients and community control subjects: a pilot study. Biol Psychiatry. 2005; 57:633–639. [PubMed: 15780850]
56. Hajek T, Cullis J, Novak T, Kopecek M, Höschl C, Blagdon R, O'Donovan C, Bauer M, Young LT, Macqueen G, Alda M. Hippocampal volumes in bipolar disorders: opposing effects of illness burden and lithium treatment. Bipolar Disord. 2012; 14:261–270. [PubMed: 22548899]
57. Hallahan B, Newell J, Soares JC, Brambilla P, Strakowski SM, Fleck DE, Kieseppä T, Altshuler LL, Fornito A, Malhi GS, McIntosh AM, Yurgelun-Todd DA, Labar KS, Sharma V, MacQueen GM, Murray RM, McDonald C. Structural magnetic resonance imaging in bipolar disorder: an international collaborative mega-analysis of individual adult patient data. Biol Psychiatry. 2011; 69:326–335. [PubMed: 21030008]
58. Vita A, De Peri L, Sacchetti E. Gray matter, white matter, brain, and intracranial volumes in first-episode bipolar disorder: a meta-analysis of magnetic resonance imaging studies. Bipolar Disord. 2009; 11:807–814. [PubMed: 19922551]
59. Cousins DA, Aribisala B, Nicol Ferrier I, Blamire AM. Lithium, gray matter, and magnetic resonance imaging signal. Biol Psychiatry. 2013; 73:652–657. [PubMed: 23158114]
60. Lyoo IK, Dager SR, Kim JE, Yoon SJ, Friedman SD, Dunner DL, Renshaw PF. Lithium-induced gray matter volume increase as a neural correlate of treatment response in bipolar disorder: a longitudinal brain imaging study. Neuropsychopharmacology. 2010; 35:1743–1750. [PubMed: 20357761]

61. Saul MC, Gessay GM, Gammie SC. A new mouse model for mania shares genetic correlates with human bipolar disorder. PLoS One. 2012; 7(6):38128.

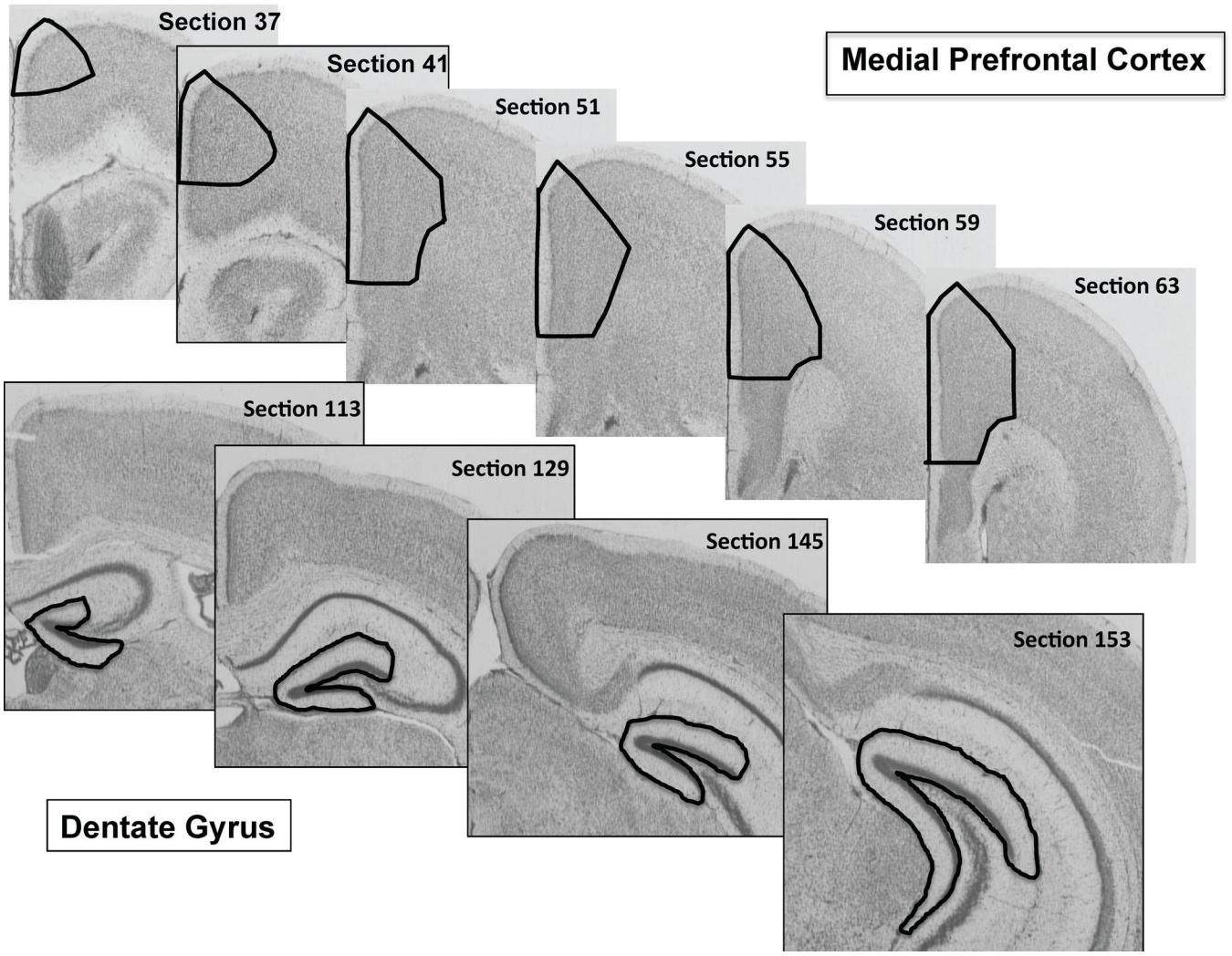

Figure 1.

Coronal sections of a representative mouse brain stained by the Nissl method taken from the medial prefrontal cortex (black contours in the upper row) and dentate gyrus of the hippocampus (black contours in the lower row). The black contours represent the entire rostral-to-caudal extent of these areas in which the total number of neurons and glial cells were counted using the optical fractionator method of StereoInvestigator software.

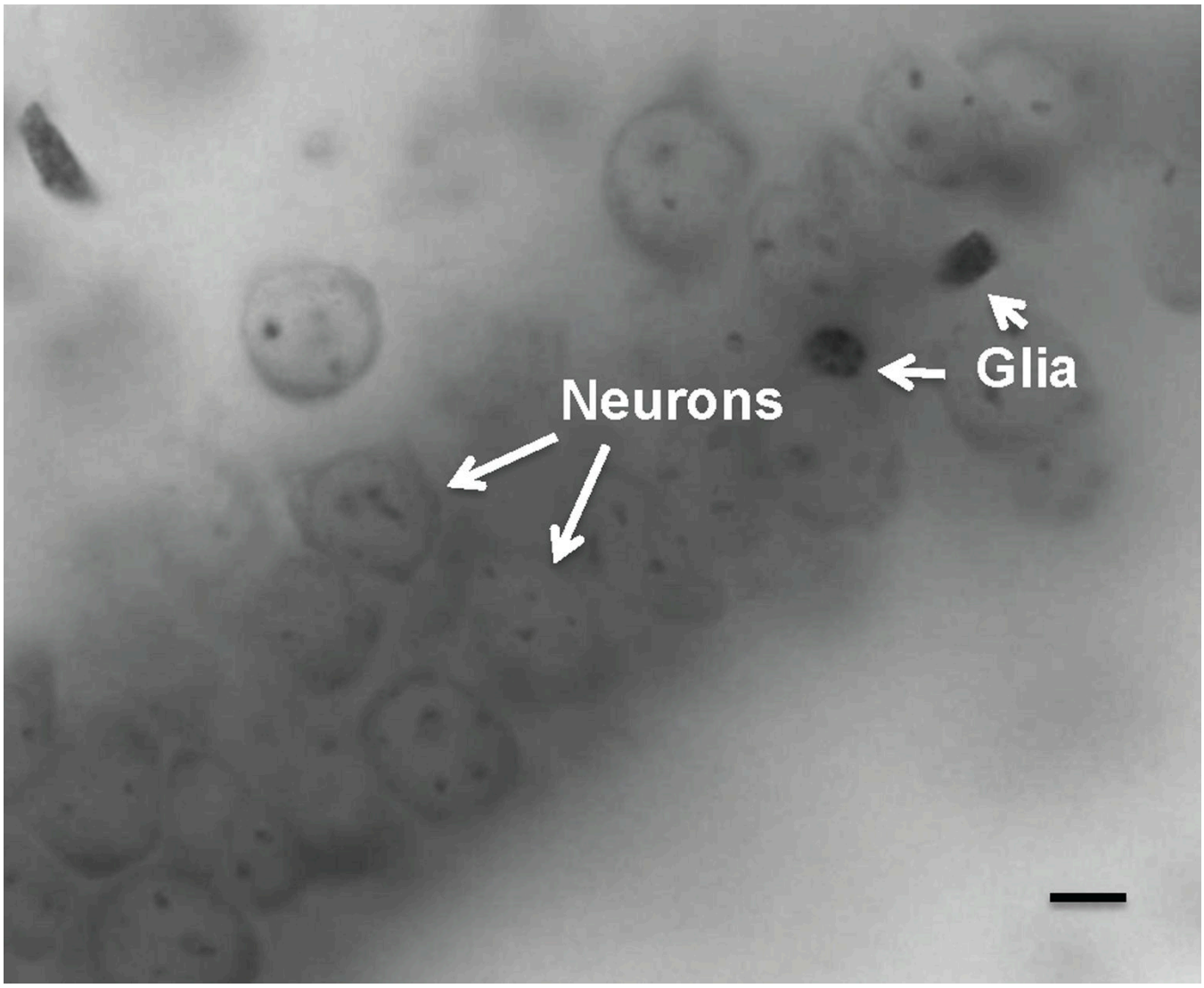

Figure 2.

Photomicrograph of Nissl-stained neurons and glial cells in the dentate gyrus of a lithium-treated mouse. Note that at high magnification (1000 X), neurons (long white arrows) can be distinguished from smaller and darker glial cells (short white arrows). Scale bar = 10μm.

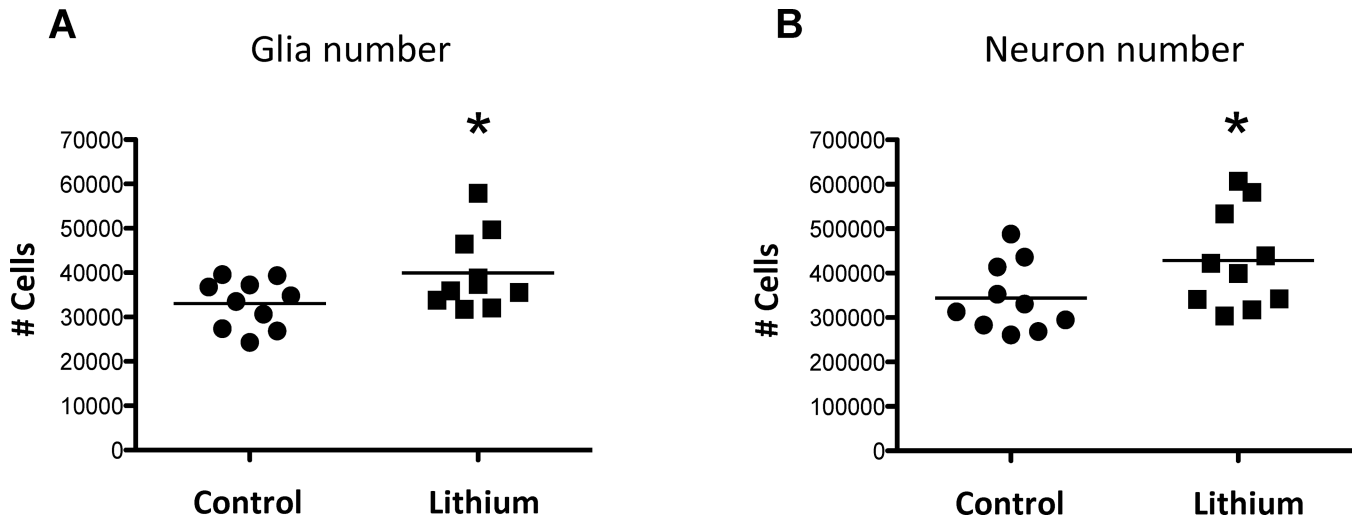

Figure 3.

Total number of glial cells (A) and neurons (B) in the dentate gyrus of lithium-treated and control mice. *p<0.05. Note significant increases in the total number of glial cells and neurons in lithium-treated versus control mice.

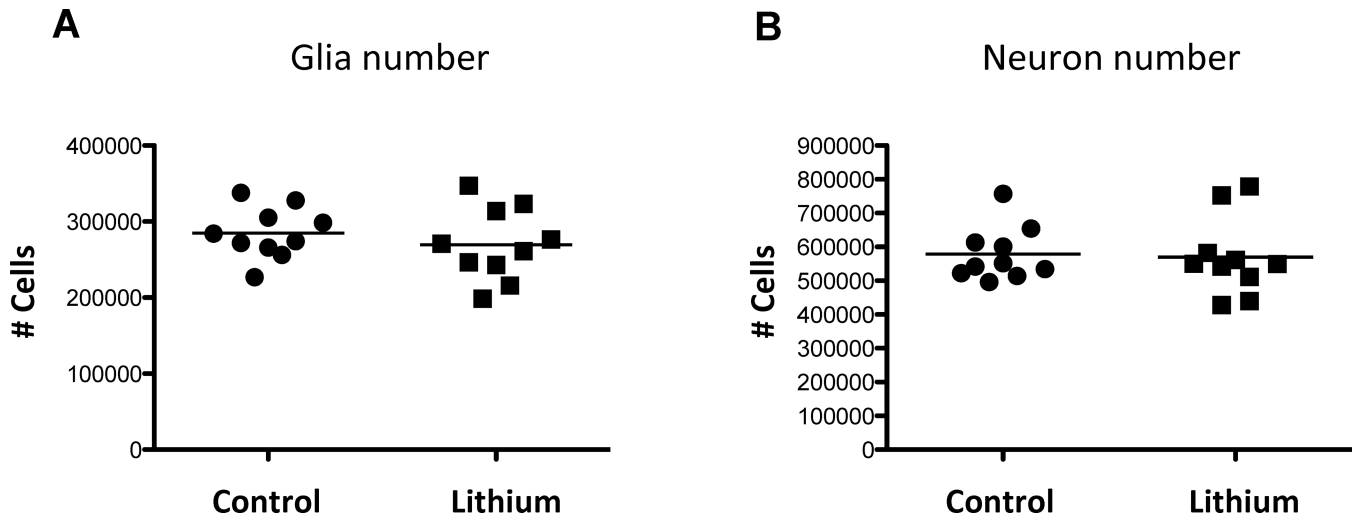

Figure 4.

Total number of glial cells (A) and neurons (B) in the medial prefrontal cortex of lithium-treated and control mice. There were no significant differences in the total number of glial cells or neurons between the two groups of mice.

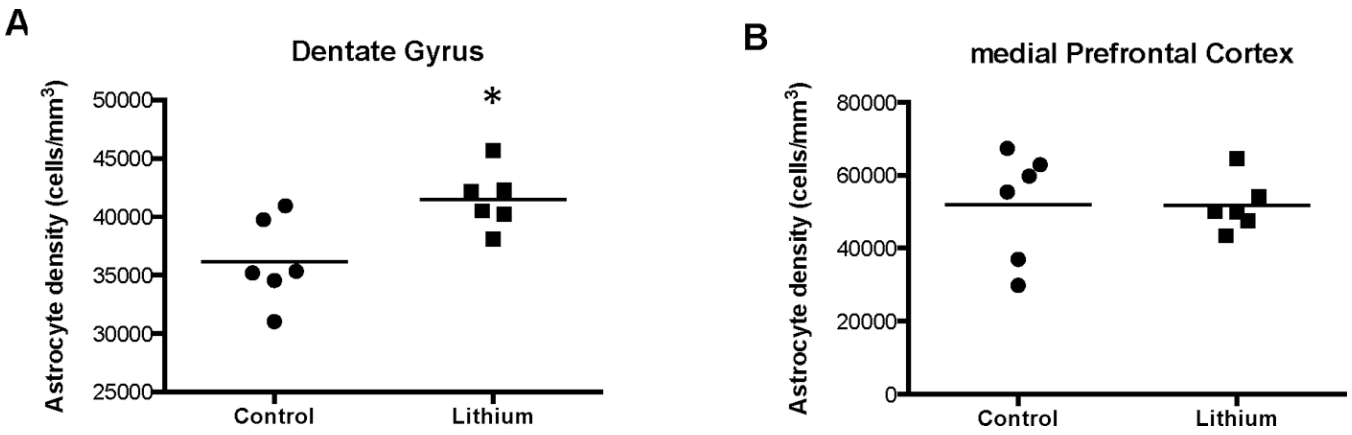

Figure 5.

Density of GFAP-immunoreactive astrocytes in the dentate gyrus (A) and the medial prefrontal cortex (B). There was a significant (*$p<0.01$) increase in the packing density of astrocytes in the dentate gyrus but not in the medial prefrontal cortex in lithium-treated versus control mice.

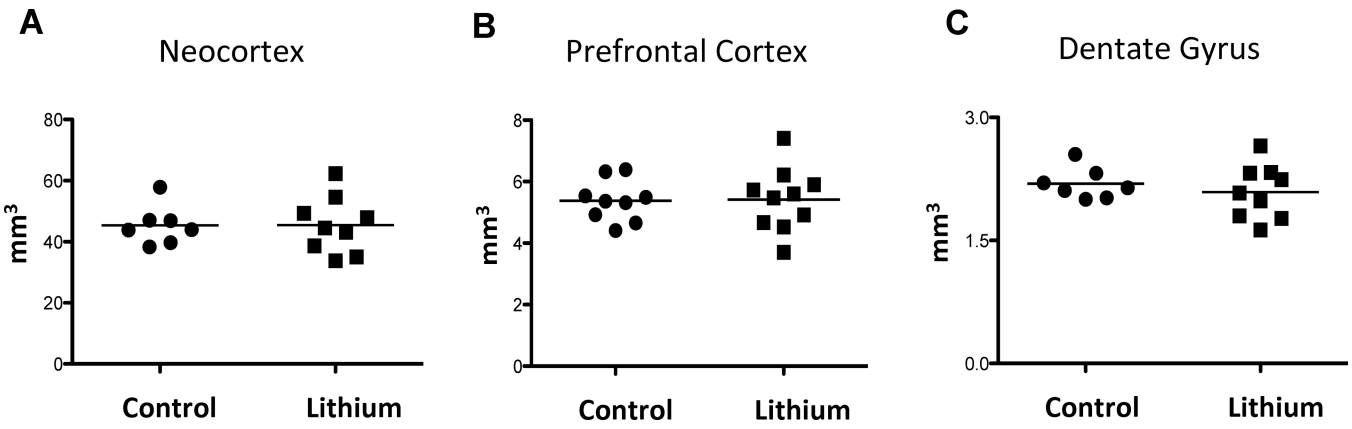

Figure 6.

Total volume of the entire right and left neocortex (A), medial prefrontal cortex (B) and dentate gyrus (C) in lithium-treated and control mice. There were no significant differences in the total volume of these brain regions between the two groups of mice.

Table 1

Cell number: dentate gyrus and medial prefrontal cortex *

Brain Region	Cell Group (n=10 each)	Mean (x10^5)	95% CI	CE	CE^2/CV^2
Dentate Gyrus					
	Neurons control	3.44	[2.89 , 4.00]	0.07	9%
	Neurons lithium	4.29	[3.49 , 5.08]	0.07	7%
	Glia control	0.330	[0.291, 0.370]	0.07	16%
	Glia lithium	0.399	[0.338, 0.461]	0.07	9%
	Medial PFC				
Neurons control		5.79	[5.24 , 6.33]	0.04	11%
	Neurons lithium	5.70	[4.91 , 6.48]	0.04	5%
	Glia control	2.85	[2.62 , 3.08]	0.06	32%
	Glia lithium	2.70	[2.37 , 3.02]	0.06	15%

*left hemisphere values

CE: Coefficient of Error; CI: Confidence Interval; CV: Coefficient of Variation (sd/mean)

Table 2

Total volume of neocortex, hippocampus and its subregions*.

Brain Region	Group	(n)	Mean (mm^3)	95% CI	CE (m=0)	CE^2/CV^2
Neocortex	control	(7)	45.4	[39.4 , 51.3]	0.04	8%
	lithium	(9)	45.1	[38.0 , 52.2]	0.04	4%
Hippocampus	control	(7)	11.19	[10.24 , 12.14]	0.01	2%
	lithium	(9)	10.73	[9.63 , 11.83]	0.01	1%
CA1	control	(7)	3.27	[2.84 , 3.69]	0.08	29%
	lithium	(9)	3.17	[2.87 , 3.47]	0.03	5%
CA2-3	control	(7)	3.24	[2.99 , 3.49]	0.07	69%
	lithium	(9)	3.01	[2.65 , 3.37]	0.05	11%
Dentate Gyrus	control	(7)	2.19	[2.01 , 2.37]	0.07	47%
	lithium	(9)	2.09	[1.84 , 2.34]	0.03	3%
Hilus	control	(7)	0.295	[0.271 , 0.320]	0.16	2.47%
	lithium	(9)	0.291	[0.265 , 0.318]	0.12	1.01%
Subiculum	control	(7)	2.20	[1.96 , 2.44]	0.12	81%
	lithium	(9)	2.17	[1.91 , 2.43]	0.05	11%

*left plus right hemisphere values

CE: Coefficient of Error (see for m=0 the text in Materials & Methods); CI: Confidence Interval; CV: Coefficient of Variation (sd/mean)

Table 3

Total volume of medial prefrontal cortex (mPFC), and its subregions*.

Brain Region	Group	(n)	Mean (mm^3)	95% CI	CE (m=0)	CE^2/CV^2
mPFC	control	(9)	5.38	[4.86 , 5.89]	0.01	< 1%
	lithium	(10)	5.41	[4.68 , 6.15]	0.01	< 1%
Fr2	control	(9)	2.81	[2.47 , 3.16]	0.02	2%
	lithium	(10)	2.80	[2.37 , 3.22]	0.03	2%
ACd	control	(9)	1.21	[1.09 , 1.34]	0.03	3%
	lithium	(10)	1.16	[0.97 , 1.35]	0.03	2%
ACv	control	(9)	0.561	[0.458 , 0.664]	0.05	5%
	lithium	(10)	0.699	[0.578 , 0.821]	0.04	3%
PL	control	(9)	0.581	[0.518 , 0.654]	0.05	9%
	lithium	(10)	0.582	[0.525 , 0.639]	0.06	18%
IL	control	(9)	0.209	[0.150 , 0.268]	0.07	3%
	lithium	(10)	0.179	[0.140 , 0.218]	0.09	9%

*left plus right hemisphere values

ACd: dorsal agranular cingulate area; ACv: ventral agranular cingulate area; CE: Coefficient of Error; CI: Confidence Interval; CV: Coefficient of Variation (sd/mean); Fr2: Frontal area 2; IL: Infralimbic area; mPFC: Medial prefrontal cortex; PL: Prelimbic area.